Supplementary Information

Cyanogroup Functionalized Sub-2 nm Ultrafine Pt Nanonetworks Reinforce Electrocatalytic Hydrogen Evolution in A Broad pH Range

Qicheng Liu,[a] Xuan Wang,[a] Jiaqi Liu,[a] Xinyi Zhou,[a] Qingwei Meng,[a] Xinrui Zhou,[a] Dongmei Sun,[a]* Yawen Tang [a]*

[a] Jiangsu Key Laboratory of New Power Batteries, Jiangsu Collaborative Innovation Centre of Biomedical Functional Materials, School of Chemistry and Materials Science, Nanjing Normal University, Nanjing 210023, China.

Emails: sundongmei@njnu.edu.cn (D. Sun); tangyawen@njnu.edu.cn (Y. Tang)

Experimental Section

Chemicals and Materials

Potassium chloroplatinate (K_2PtCl_4) was purchased from DB Biotechnology Co., Ltd. (Shanghai, China). Cyanoacetic acid (CAA), ethylene glycol (EG), diethylene glycol (DEG) and triethylene glycol (TEG) were purchased from Aladdin Co., Ltd (Shanghai. China). Absolute ethyl alcohol (C_2H_5OH), sodium hydroxide (NaOH), potassium hydroxide (KOH), perchloric acid ($HClO_4$), sodium borohydride ($NaBH_4$), sodium cyanoborohydride ($NaBH_3CN$, SC), acetone (C_3H_6O) and N, N-dimethylformamide (DMF) were purchased from Sinopharm Chemical Reagent Co., Ltd (Shanghai, China). 20wt% Pt/C was purchased from Johnson Matthey Corporation. All the reagents were not further purified before use.

Synthesis of the CN-Pt Ultrafine Nanonetworks (UNs)

In a typical synthesis, 0.5 mL K_2PtCl_4 (0.05 M) and 0.5 mL CAA were added to 5 mL EG in a vial (volume: 20 mL) with continuous string. After stirring thoroughly, 0.25 mL 0.05 M SC and 0.25 mL 0.05 M NaOH aqueous solution was added into the reaction system. Then, the mixed solution was kept under 120 ℃ in oil bath for 1 h. Finally, the CN-Pt UNs were separated by centrifugation at 15,000 rpm for 6 min and washed several times with deionized (DI) water. Finally, the acquired product was dried in the vacuum freeze dryer at 70 ℃ for 24 h.

Synthesis of the SC-Pt Nanoparticles (NPs) and CAA-Pt Nanonetworks (NNs)

The synthetic procedures of SC-Pt NPs and CAA-Pt NPs were similar to that of CN-Pt UNs except for no adding CAA and replacing SC with 0.5 mL 0.1 M $NaBH_4$, respectively.

Synthesis of the Pt-DEG UNs and Pt-TEG UNs

Pt-DEG UNs and Pt-TEG UNs were synthesized via the same synthetic procedure of CN-Pt UNs except for using DEG and TEG to replace EG, respectively.

Synthesis of the Pt-water and Pt-DMF NPs

Pt-water NPs and Pt-DMF NPs were synthesized via the same synthetic procedure of CN-Pt UNs except for using DI water and DMF to replace EG, respectively.

Physicochemical Characterization

Transmission electron microscopy (TEM) and high-resolution TEM (HRTEM) images were characterized on a JEOL JEM-2100F transmission electron microscopy with an accelerating voltage of 200 kV. High-angle annular dark-field scanning TEM (HAADF-STEM) images were acquired on JEOL JEM-ARM 200F. Fourier Transform-

Infrared (FT-IR) spectra were obtained on a Bruker Vertex 70 FTIR spectrometer to verify the successful modification of cyanogroup on the CN-Pt UNs. XPS measurements were conducted on a Thermo VG Scientific ESCALAB 250 spectrometers with an Al Kα radiator. The binding energy was calibrated by means of the C 1s peak energy of 284.6 eV. XRD analysis was performed on a Model D/max-rC X-ray diffractometer employing Cu Kα radiation (λ = 0.15406 nm) and operating at 40 kV and 100 mA. The N_2 adsorption-desorption isotherms were measured at 77K on a Belsorp-Max surface area analyser (Belsorp-Max, MicrotracBEL, Japan).

Electrochemical Measurements

Electrochemical measurements were performed on a CHI 760E CH analyser (Shanghai, Chenhua Co.) with a conventional three-electrode system. 4.0 mg of electrocatalysts were dispersed into a mixture of 0.7 mL of alcohol, 1.2 mL of deionized water and 0.1 mL of Nafion solution (5 wt%) and the above substances were mixed by sonication thoroughly for 30 min. Then, 20 μL of the acquired catalyst ink (2 mg mL^{-1}) was dropped onto the surface of the glass carbon electrode of 3.0 mm diameter, thus the mass loading of the catalyst on the GC electrode is 0.567 mg cm^{-2}. The glassy carbon electrode loaded with catalyst was used as the working electrode, the graphite rod as the counter electrode, and the saturated calomel electrode (SCE) as the reference electrode for the HER tests. All potentials reported in this work were transformed to the reversible hydrogen electrode (RHE), and the conversion formulas were as follows: $E_{RHE} = E_{SCE} + 0.0592$ pH + 0.242 V. All the hydrogen evolution reaction (HER) polarization curves were acquired via the linear sweep voltammetry (LSV) measurement at a scan rate of 5 mV s^{-1} in N_2-saturated 1.0 M KOH or 1.0 M $HClO_4$ solution. The electrochemical stability test was investigated by the chronoamperometric curves under the constant potentials at 10 mA cm^{-2}.
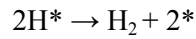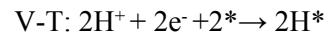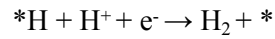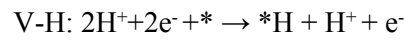
DFT Calculations

Density functional theory (DFT) was operated with Vienna ab initio simulation package (VASP) with projector augmented plane wave (PAW) potentials.[1] The Perdew-Burke-Ernzerhof (PBE) functional of the generalized gradient approximation (GGA) was selected to describe the Kohn-Sham exchange-correlation functional.[2] The DFT-D3 method by Grimme was adopted in our work.[3] The cut-off energy of the plane wave basis was set to be 400 eV. To balance the calculation cost and precision, the whole model used in our work was comprised of 14 atoms, as shown in Fig. S1. The 5 × 5 × 1 k-point mesh was chosen to sample the Brillouin zone, and a 15 Å vacuum was introduced to avoid the interaction between the repeated slabs along the z direction. The whole model was relaxed until the residual force was less than 0.02 eV Å^{-1}.

The absorption free energy of absorbates in HER can be calculated as the following formula:

$$\Delta G_{abs} = \Delta E_{abs} + \Delta(ZPE) - \Delta(TS)$$

Where ΔE_{abs} is the absorption energy of absorbates, $\Delta(ZPE)$ is the zero-point energy, T is the absolute temperature, and S is the entropy. As developed by Nørskov et al, computational hydrogen electrode (CHE) was used to calculate the free energy of the combination of proton and electron in elemental steps in HER.[4] According to CHE, at the bias potential of U=0 V and the standard concentration of H^+, the free energy of H^+ + e^- can be described as $\Delta G(H^+) + \Delta G(e^-) = \frac{1}{2}\Delta G(H_2)$. Hence, the free energy change during Volmer-Heyrovsky (V-H) and Volmer-Tafel (V-T) mechanism can be expressed as:
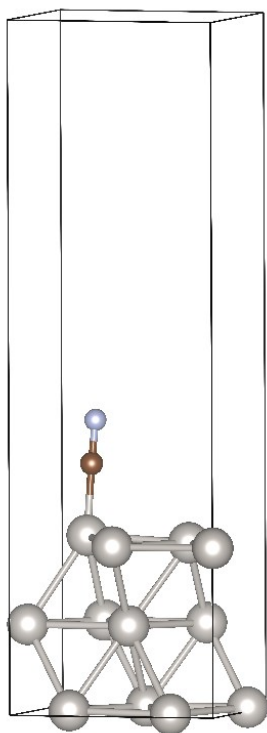
$$V\text{-}H: 2H^+ + 2e^- + * \rightarrow *H + H^+ + e^-$$

$$*H + H^+ + e^- \rightarrow H_2 + *$$

$$V\text{-}T: 2H^+ + 2e^- + 2* \rightarrow 2H*$$

$$2H* \rightarrow H_2 + 2*$$

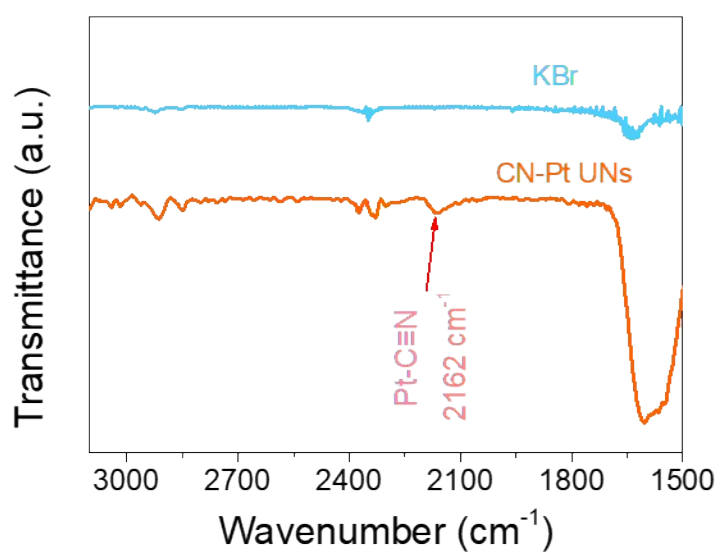Where $\Delta G(*H)$ is $\Delta G(*H) = \Delta E(*H) + \Delta(ZPE) - \Delta(TS)$, and $\Delta E(*H)$ can be expressed as:

$$\Delta E(*H) = E(*H) - E(*) - \frac{1}{2}E(H_2).$$
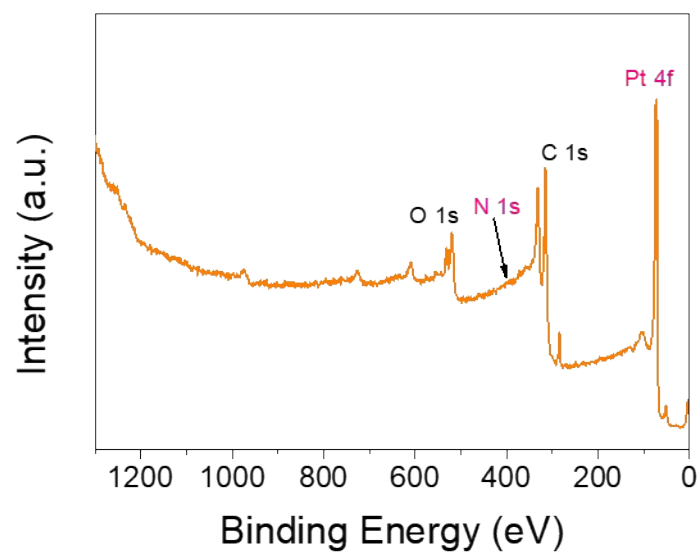
The * in above formulas denotes the slab model.
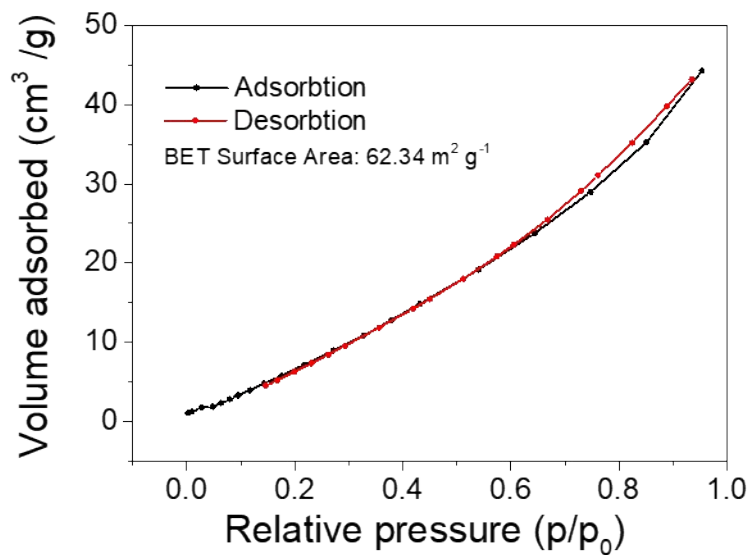
Figures and Tables

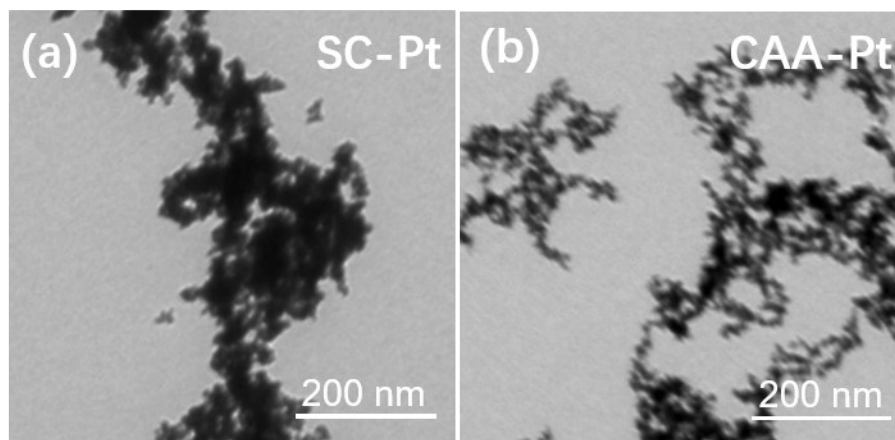

Figure S1. Geo-optimized model of CN-Pt UNs.

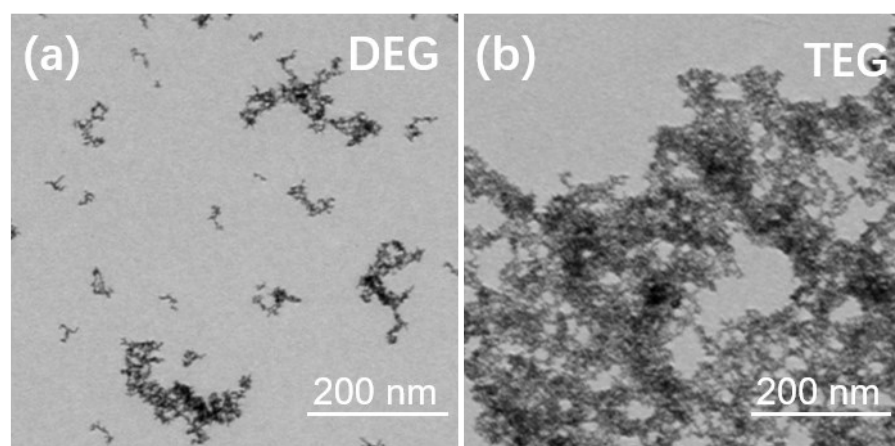**Figure S2.** FT-IR spectrum of CN-Pt UNs.

Figure S3. XPS survey scan spectrum of CN-Pt UNs.
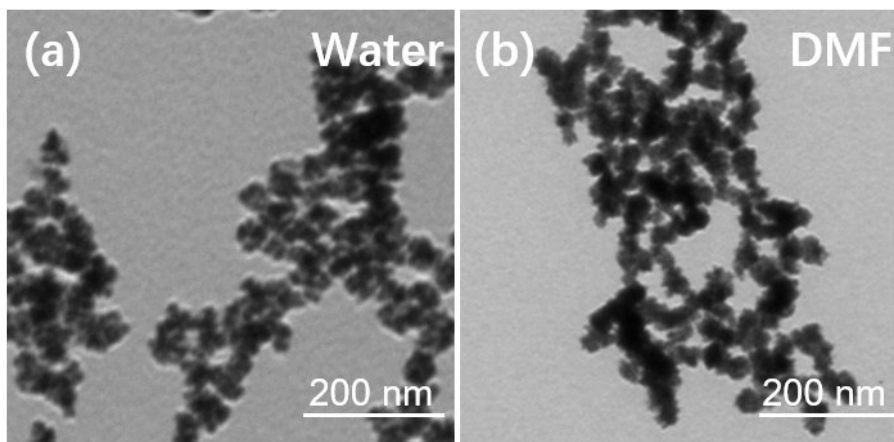

Figure S4. N_2 adsorption-desorption isotherms of CN-Pt UNs.

Figure S5. TEM images of (a) SC-Pt NPs and (b) CAA-Pt NNs.

Figure S6. TEM images of Pt-DEG UNs and Pt-TEG UNs.

Figure S7. TEM images of (a) Pt-water NPs and (b) Pt-DMF NPs.
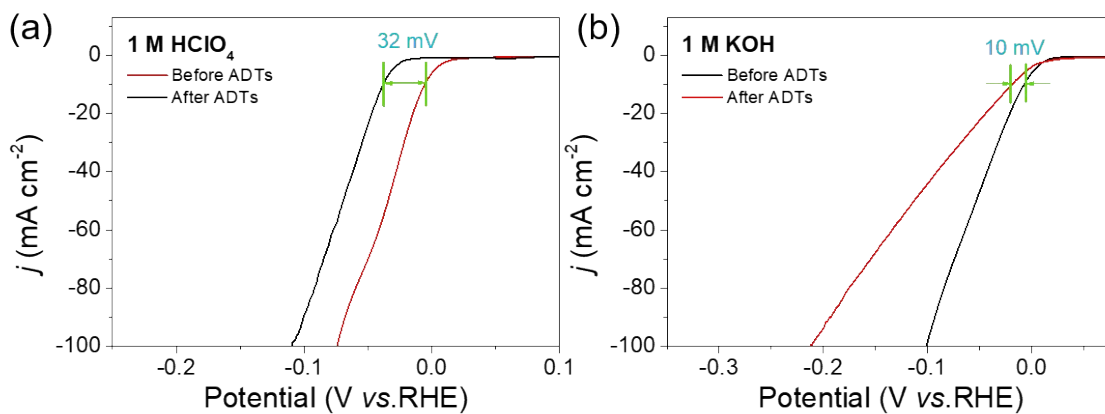
Figure S8. The HER polarization curves of CN-Pt UNs before and after ADTs of 1,000 circles in (a) 1 M HClO$_4$ and (b) 1 M KOH.

Figure S9. TEM images of CN-Pt UNs after ADTs of 1,000 circles in (a) 1 M HClO$_4$ and (b) 1 M KOH.

Figure S10. XRD patterns of CN-Pt UNs before and after ADTs of 1,000 circles.

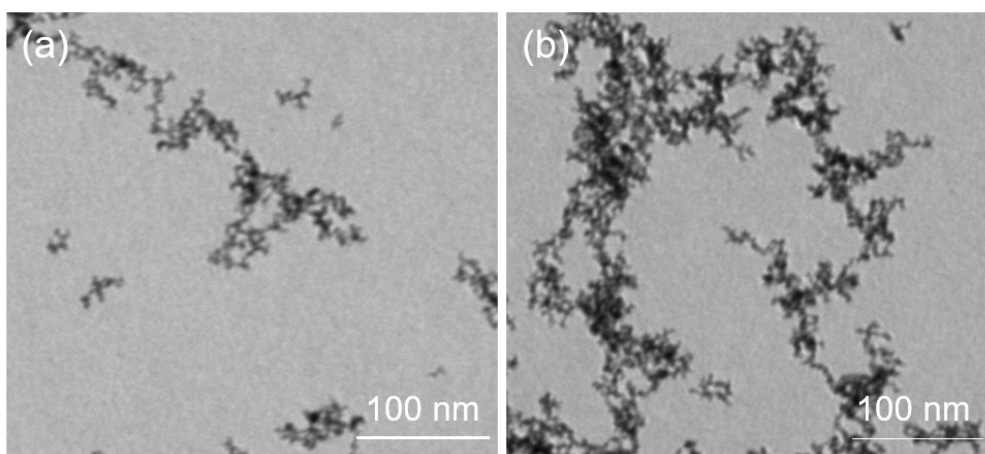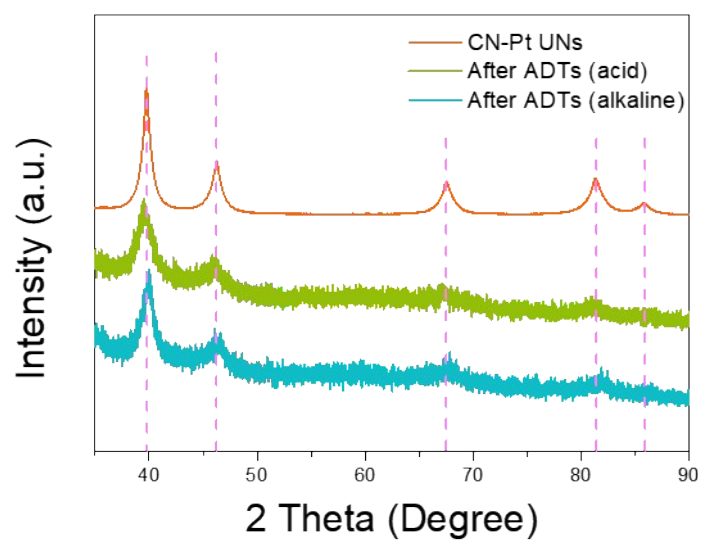**Table S1.** Comparison of relevant metal electrocatalysts for the HER reported before. (Alkaline)

Catalysis	Electrolyte	Overpotential (mV)	Tafel Slope (mV dec^{-1})	Reference
CN-Pt UNs	1 M KOH	8	26.9	This Work
Rh$_2$Ir NDs	1 M KOH	9	25.8	5
PdPtCuNiP	1 M KOH	32	37.4	6
IrRh sheet	1 M KOH	35	48.4	7
CoPt-NC	1 M KOH	50	48	8
RhO$_2$ particle	1 M KOH	14	30	9
Rh@NG	0.1 M KOH	45	30	10
Rh-Si	1 M KOH	130	24	11
Ir$_4$Ru	1 M NaOH	32	32.9	12
Pt$_{18}$Ni$_{26}$Fe$_{15}$Co$_{14}$Cu$_{27}$/C	1 M KOH	11	30	13
Ru/CoO	1 M KOH	55	70	14
SA-Ru/Ru NPs/PC	1 M KOH	33	29	15
Pd–Ru@NG	1 M KOH	28	42	16
Ru/amorphous C	1 M KOH	53	47	17

Table S2. Comparison of relevant metal electrocatalysts for the HER reported before. (Acid)

Catalysis	Electrolyte	Overpotential (mV)	Tafel Slope (mV dec^{-1})	Reference
CN-Pt UNs	1 M HClO$_4$	6	42.3	This Work
Rh$_2$Ir NDs	1 M HClO$_4$	12	17.3	5
Hollow Pt NPs	0.5 M H$_2$SO$_4$	37	31	18
CoPt-NC	0.5 M H$_2$SO$_4$	27	31	8
Ru Nanosheet	0.5 M H$_2$SO$_4$	20	46	19
Rh@NG	0.5 M H$_2$SO$_4$	29	30	10
Ru/amorphous C	0.5 M H$_2$SO$_4$	35	36.2	17
PtCoIr NWs	0.1 M HClO$_4$	14	～	20
IrCo NFs	0.1 M HClO$_4$	24	35.3	21
IrCo/C	0.1 M HClO$_4$	24	26.6	22
Pd–Ru@NG	1 M H$_2$SO$_4$	39	60	16

References

1.   G. Kresse and J. Furthmüller, *Phys. Rev. B*, 1996, **54**, 11169-11186.

2.   J. P. Perdew, Kieron Burke and M. Ernzerhof, *Phys. Rev. Lett.*, 1996, **77**, 3865-3868.

3.   S. Grimme, *J. Comput. Chem.*, 2006, **27**, 1787-1799.

4.   J. K. Norskov, J. Rossmeisl, A. Logadottir, L.Lindqvist, J. R. Kitchin, T. Bligaard and H. Jonsson, *J. Phys. Chem. B* 2004, **108**, 17886-17892.

5.   Q. Liu, C. Fan, X. Zhou, J. Liu, S. Jiang, S. Wang, X. Wang and Y. Tang, *New J. Chem.*, 2020, **44**, 21021-21025.

6.   Z. Jia, K. Nomoto, Q. Wang, C. Kong, L. Sun, L. C. Zhang, S. X. Liang, J. Lu and J. J. Kruzic, *Adv. Funct. Mater.*, 2021, DOI: 10.1002/adfm.202101586.

7.   C. Li, Y. Xu, S. Liu, S. Yin, H. Yu, Z. Wang, X. Li, L. Wang and H. Wang, *Acs Sustain. Chem. Eng.*, 2019, **7**, 15747-15754.

8.   L. Zhang, Y. Jia, H. Liu, L. Zhuang, X. Yan, C. Lang, X. Wang, D. Yang, K. Huang, S. Feng and X. Yao, *Angew. Chem. Int. Ed.*, 2019, **58**, 9404-9408.

9.   Z. Li, Y. Feng, Y. L. Liang, C. Q. Cheng, C. K. Dong, H. Liu and X. W. Du, *Adv. Mater.*, 2020, **32**, 1908521.

10.   J. Guan, X. Wen, Q. Zhang and Z. Duan, *Carbon*, 2020, **164**, 121-128.

11.   L. Zhu, H. Lin, Y. Li, F. Liao, Y. Lifshitz, M. Sheng, S. T. Lee and M. Shao, *Nat. Commun.*, 2016, **7**, 12272.

12.   Y. B. Cho, A. Yu, C. Lee, M. H. Kim and Y. Lee, *ACS Appl. Mater. Interfaces*, 2018, **10**, 541-549.

13.   H. Li, Y. Han, H. Zhao, W. Qi, D. Zhang, Y. Yu, W. Cai, S. Li, J. Lai, B. Huang and L. Wang, *Nat. Commun.*, 2020, **11**, 5437.

14.   J.-X. Guo, D.-Y. Yan, K.-W. Qiu, C. Mu, D. Jiao, J. Mao, H. Wang and T. Ling, *J. Energy Chem.*, 2019, **37**, 143-147.

15.   Q. Hu, G. Li, X. Huang, Z. Wang, H. Yang, Q. Zhang, J. Liu and C. He, *J Mater. Chem. A*, 2019, **7**, 19531-19538.

16.   B. K. Barman, B. Sarkar and K. K. Nanda, *Chem. Commun.*, 2019, **55**, 13928-13931.

17.   Y. Li, J. Abbott, Y. Sun, J. Sun, Y. Du, X. Han, G. Wu and P. Xu, *Appl. Catal. B*, 2019, **258**.

18.   Y. Wang, S. Ma, Q. Li, Y. Zhang, X. Wang and X. Han, *Acs Sustain. Chem. Eng.*, 2016, **4**, 3773-3779.

19.   X. Kong, K. Xu, C. Zhang, J. Dai, S. Norooz Oliaee, L. Li, X. Zeng, C. Wu and Z. Peng, *Acs Catal.*, 2016, **6**, 1487-1492.

20.   Y. Sun, B. Huang, Y. Li, Y. Xing, M. Luo, N. Li, Z. Xia, Y. Qin, D. Su, L. Wang and S. Guo, *Chem. Mater.*, 2019, **31**, 8136-8144.

21.   L. Fu, X. Zeng, G. Cheng and W. Luo, *ACS Appl. Mater. Interfaces*, 2018, **10**, 24993-24998.

22.   J. Feng, F. Lv, W. Zhang, P. Li, K. Wang, C. Yang, B. Wang, Y. Yang, J. Zhou, F. Lin, G. C. Wang and S. Guo, *Adv. Mater.*, 2017, **29**, 1703798.